

Neural Networks Assisted Metropolis-Hastings for Bayesian Estimation of Critical Exponent on Elliptic Black Hole Solution in 4D Using Quantum Perturbation Theory

Armin Hatefi^{*1}, Ehsan Hatefi^{†2}, and R. J. Lopez-Sastre^{‡3}

¹Department of Mathematics and Statistics, Memorial University
of Newfoundland, St. John's, NL, Canada.

^{2,3}University of Alcalá, Department of Signal Theory and
Communications, Research group GRAM, Alcalá de Henares,
Spain.

June 7, 2024

Abstract: The critical gravitational collapse is known to produce continuous self-similar solutions characterized by the Choptuik critical exponent, γ . We examine all solutions within the complete domains of the linear perturbation equations, considering the numerical measurement errors. Specifically, we study quantum perturbation theory for the four-dimensional Einstein-axion-dilaton system of the elliptic class of $SL(2, \mathbb{R})$ transformations. We developed a novel artificial neural network-assisted Metropolis-Hastings based on quantum perturbation theory to find the critical exponent in a Bayesian framework. Unlike existing methods, this new probabilistic approach identifies the available deterministic solutions and explores the range of physically distinguishable critical exponents that may arise due to numerical measurement errors.

^{*}ahatefi@mun.ca

[†]ehsan.hatefi@uah.es

[‡]roberto.j.lopez@uah.es

1 Introduction

Black holes are known to be the final state of gravitational collapse. They do have a well-known characteristic property, that is, they are entirely defined by mass, angular momentum, and charge. Choptuik revealed in [1] that there seems to be another parameter or the fourth quantity that establishes the collapse itself. Building on Christodoulou's study in [2] for the spherically symmetric collapse of scalar fields, Choptuik explored that a critical behavior shows discrete spacetime self-similarity. By evaluating the amplitude of the scalar field fluctuation as p , he discovered that p must be greater than the critical value p_{crit} to form a black hole. Moreover, for values of p above this threshold, the mass of the black hole M_{bh} results a scaling law as follows

$$r_S(p) \propto M_{\text{bh}}(p) \propto (p - p_{\text{crit}})^\gamma, \quad (1)$$

The critical exponent in 4d for a single real scalar field is given by $\gamma \simeq 0.37$ [1, 3, 4], while for general dimension ($d \geq 4$) [5, 6] these relations get modified as follows

$$r_S(p) \propto (p - p_{\text{crit}})^\gamma, \quad M_{\text{bh}}(p) \sim (p - p_{\text{crit}})^{(D-3)\gamma}. \quad (2)$$

Various numerical simulations with other fields are carried out [7, 8, 9, 10, 11, 12]. As an instance the collapse of a perfect fluid is done in [13, 14, 5, 15]. In [14] they explored $\gamma \simeq 0.36$ and therefore it was realised in [16] that γ might be universal for all matter field coupled to gravity in four dimensions. It was first in [5, 15, 17] that the authors found the critical exponent may be found by working out the perturbations of the solutions. To achieve the perturbations, one needs to perturb any field h (be it the metric or the matter content) as the following

$$h = h_0 + \varepsilon h_{-\kappa} \quad (3)$$

where the perturbation $h_{-\kappa}$ does have the scaling $-\kappa \in \mathbb{C}$ that labels the different modes. Inside the allowed values of κ , we express the most relevant mode κ^* to be the highest value of $\text{Re}(\kappa)$. In [5, 15, 17] it was argued that the κ^* is related to the critical exponent by $\gamma = \frac{1}{\text{Re} \kappa^*}$. The axial symmetry was analysed in [18] and the critical solution for the shock waves was known in [19]. For the first time the axion-dilaton critical collapse solution coupled to gravity in four dimension was determined in [20] where they found the value $\gamma \simeq 0.2641$,

hence arguing the doubts relating the universality of γ in four dimension.

The first motivation for studying critical solutions in the axion-dilaton system is the AdS/CFT correspondence [21], which relates the Choptuik exponent to the imaginary part of quasi normal modes and the dual conformal field theory [22]. Additional motivations include the holographic description of black hole formation [6] and the broader physics of black holes and their applications to holography and string theory [23, 24].

In type IIB string theory, there is significant interest in exploring gravitational collapse in spaces that can asymptotically approach $AdS_5 \times S^5$, where the matter content describes by the axion-dilaton system and the self-dual 5-form field. Entire families of distinguishable continuous self-similar solutions of the Einstein-axion-dilaton system in four and five dimensions, for all three conjugacy classes of $SL(2, \mathbb{R})$, were recently explored in [25], generalizing previous efforts made in [26, 27]. Utilizing robust analytic and numerical techniques from [28], we perturbed the critical solution of four-dimensional elliptic critical collapse and successfully recovered the known value of $\gamma \sim 0.2641$ [20]. This achievement provides strong confidence in our ability to determine other critical exponents across different dimensions and for various classes of solutions.

In [29] we have imposed the regression models for the nonlinear critical functions. To address these challenges in [30] we worked out various methods such as truncated power basis, natural spline and penalized B-spline regression models to be able to estimate the non-linear functions that appear in the physics of black holes for the particular axion-dilaton case. Very recently, in [31] we also started dealing with applied artificial neural networks to address in details the analysis of the black hole solutions in parabolic class in higher dimensions as well. Furthermore, in [32] we dealt with a new methodology that can be employed to work with the problem of the complexity of elliptical black holes by making use of the so called Bayesian statistical modeling. Finally in [33] we applied the sequential Monte Carlo approach to explore the multi-modal posterior distributions. Indeed this probabilistic perspective enables us not only to determine the available solutions in the literature but also finds out all the possible solutions that might have occurred due to measurement errors.

In this paper, first we provide a brief recap on Einstein-axion-dilaton system, then we establish all the linear perturbation analysis for the elliptic case in 4d

that will enable us to extract the entire range of the critical exponent. The new methodology we employ is quite generic and can be applied to other matter contents as well.

Here we would like to investigate a generic formalism based on Neural Networks Assisted Metropolis-Hastings to obtain the entire range of possible values of critical exponents. We apply the method of Bayesian estimation of critical Exponent on elliptic Black Hole solution in 4D using quantum perturbation theory and extract the Choptuik exponent in its entire domain and in particular we explore its entire range of values for 4d elliptic black hole solution of the Einstein-axion-dilaton system. Indeed, unlike the literature, here we explore the whole (possible) range of possible values of critical exponents based on quantum perturbation theory. In fact we have analysed not only based on the perturbed variables $b_1(z)$, the perturbed variables $f_{1m}(z)$ but also on analysing variable of both $b_1(z), f_{1m}(z)$ equations simultaneously, to actually accept or reject the transitions under the Uniform prior distribution. Unlike methods in the literature, not only this new probabilistic approach provides us the available deterministic solution but also explore the entire range of physically distinguishable critical exponents that might occur due to numerical measurement errors.

2 The Einstein-axion-dilaton System

The Einstein-axion-dilaton system coupled to gravity in d dimensions is defined by the following action:

$$S = \int d^d x \sqrt{-g} \left(R - \frac{1}{2} \frac{\partial_a \tau \partial^a \bar{\tau}}{(\text{Im } \tau)^2} \right). \quad (4)$$

which is known by the effective action of type II string theory [34, 35]. The axion-dilaton is expressed by $\tau \equiv a + ie^{-\phi}$. This action enjoys the $\text{SL}(2, \mathbb{R})$ symmetry as follows

$$\tau \rightarrow M\tau \equiv \frac{\alpha\tau + \beta}{\gamma\tau + \delta}, \quad (5)$$

where $\alpha, \beta, \gamma, \delta$ are real parameters satisfying $\alpha\delta - \beta\gamma = 1$. If the quantum effects are considered then the $\text{SL}(2, \mathbb{R})$ symmetry gets exchanged to $\text{SL}(2, \mathbb{Z})$ and this S-duality was revealed to be the non-perturbative symmetry of IIB string theory [36, 37, 38]. Taking the above action, one derives the equations of

motion as follows

$$R_{ab} = \tilde{T}_{ab} \equiv \frac{1}{4(\text{Im } \tau)^2} (\partial_a \tau \partial_b \bar{\tau} + \partial_a \bar{\tau} \partial_b \tau), \quad (6)$$

$$\nabla^a \nabla_a \tau + \frac{i \nabla^a \tau \nabla_a \bar{\tau}}{\text{Im } \tau} = 0. \quad (7)$$

We take the spherical symmetry for both background and perturbations and the general form of the metric in d dimensions is

$$ds^2 = (1 + u(t, r))(-b(t, r)^2 dt^2 + dr^2) + r^2 d\Omega_{d-2}^2, \quad (8)$$

$$\tau = \tau(t, r) \quad (9)$$

The angular part of the metric in d dimensions is $d\Omega_{d-2}^2$. One is able to find out a scale invariant solution by requiring the fact that under a scale transformation $(t, r) \rightarrow (\Lambda t, \Lambda r)$ so that the line element can be changed as $ds^2 \rightarrow \Lambda^2 ds^2$. Hence all the functions must be scale invariant, i.e. $u(t, r) = u(z)$, $b(t, r) = b(z)$, $z \equiv -r/t$. The effective action (4) is invariant under the $\text{SL}(2, \mathbb{R})$ transformation (5), hence τ also does need to be invariant up to an $\text{SL}(2, \mathbb{R})$ transformation, which means that if the following holds

$$\tau(\Lambda t, \Lambda r) = M(\Lambda) \tau(t, r). \quad (10)$$

then we call a system of (g, τ) , respects the above properties of a continuous self-similar (CSS) solution. It is worth highlighting that various cases get related to other classes of $\frac{dM}{d\Lambda}|_{\Lambda=1}$ [25]. Hence, τ can take three different forms [26], called elliptic, hyperbolic and parabolic cases. In this paper we deal with the elliptic ansatz and its form for axion-dilaton case can be cast as follows

$$\tau(t, r) = i \frac{1 - (-t)^{i\omega} f(z)}{1 + (-t)^{i\omega} f(z)}, \quad (11)$$

where ω is a real parameter to be known and the function $f(z)$ needs to satisfy $|f(z)| < 1$ for the elliptic case. By replacing the CSS ansätze in the equations of motion we would be able to get a differential system of equations for $u(z)$, $b(z)$, $f(z)$. Making use of spherical symmetry one can show that $u(z)$, $u'(z)$ can be expressed in terms of $b(z)$ and $f(z)$ so that finally we are left with some

ordinary differential equations (ODEs) as follows

$$b'(z) = B(b(z), f(z), f'(z)), \quad (12)$$

$$f''(z) = F(b(z), f(z), f'(z)). \quad (13)$$

These equations in 4d and in elliptic case can be written in a closed form as follows

$$\begin{aligned} 0 &= b' + \frac{z(b^2 - z^2)}{b(-1 + |f|^2)^2} f' \bar{f}' - \frac{i\omega(b^2 - z^2)}{b(-1 + |f|^2)^2} (f \bar{f}' - \bar{f} f') - \frac{\omega^2 z |f|^2}{b(-1 + |f|^2)^2}, \\ 0 &= f'' - \frac{z(b^2 + z^2)}{b^2(-1 + |f|^2)^2} f'^2 \bar{f}' + \frac{2}{(1 - |f|^2)} \left(1 - \frac{i\omega(b^2 + z^2)}{2b^2(1 - |f|^2)} \right) \bar{f} f'^2 \\ &\quad + \frac{i\omega(b^2 + 2z^2)}{b^2(-1 + |f|^2)^2} f f' \bar{f}' + \frac{2}{z} \left(1 + \frac{i\omega z^2(1 + |f|^2)}{(b^2 - z^2)(1 - |f|^2)} \right. \\ &\quad \left. + \frac{\omega^2 z^4 |f|^2}{b^2(b^2 - z^2)(1 - |f|^2)^2} \right) f' + \frac{\omega^2 z}{b^2(-1 + |f|^2)^2} f'^2 \bar{f}' + \\ &\quad \frac{2i\omega}{(b^2 - z^2)} \left(\frac{1}{2} - \frac{i\omega(1 + |f|^2)}{2(1 - |f|^2)} - \frac{\omega^2 z^2 |f|^2}{2b^2(-1 + |f|^2)^2} \right) f. \end{aligned} \quad (14)$$

The above equations have five singularities [26] located at $z = \pm 0$, $z = \infty$ and $z = z_{\pm}$ where the last singularities are known by $b(z_{\pm}) = \pm z_{\pm}$. The $z = z_+$ is just a mere coordinate singularity [20, 26], thus τ should have been regular across it and this constraint actually translates to having the finite value for $f''(z)$ as $z \rightarrow z_+$.

One actually can realise that the vanishing of the divergent part of $f''(z)$ provides us an equation that is complex valued constraint at z_+ which can be indicated by $G(b(z_+), f(z_+), f'(z_+)) = 0$ where the final form of G for the elliptic class is given as [25]

$$\begin{aligned} G(f(z_+), f'(z_+)) &= 2z \bar{f}(z_+) (-2\omega^2) f'(z_+) \\ &\quad + f(z_+) \bar{f}(z_+) (2z_+ \bar{f}(z_+) (-2 + 2i\omega + 2) f'(z_+) + 2i\omega (2 + \omega^2)) \\ &\quad - \frac{2z_+(2 + 2i\omega - 2) f'(z_+)}{f(z_+)} \\ &\quad + 2\omega(\omega - i) f(z_+)^2 \bar{f}(z_+)^2 - 2\omega(\omega + i). \end{aligned} \quad (15)$$

The initial conditions are known by the smoothness of the solution. By applying polar coordinate as $f(z) = f_m(z) e^{i f_a(z)}$, we can see that all equations are invariant under a global redefinition of the phase of $f(z)$, so this means that

$f_a(0) = 0$. Having set the regularity condition at $z = 0$ and making use of the residual symmetries in the equations of motions (14), we reveal the initial boundary conditions of the equations of motion as follows

$$b(0) = 1, f_m(0) = x_0, \quad f'_m(0) = f'_a(0) = f_a(0) = 0 \quad (16)$$

where x_0 is a real parameter and ($0 < x_0 < 1$). Therefore, we have two constraints (the vanishing of the real and imaginary parts of G) and two parameters (ω, x_0). The discrete solution in four dimensions was found in [28]. Note that these solutions are explicitly found by root-finding procedure as well as numerically integrating all the equations of motion. For instance, the solution in 4d elliptic case was discovered to be [39, 26] as

$$\omega = 1.176, \quad |f(0)| = 0.892, \quad z_+ = 2.605 \quad (17)$$

where the black hole solutions in higher dimensions for the axion-dilaton system are obtained in [40].

3 Quantum Perturbation Analysis

In this section we would like to derive the perturbation equations for black holes in elliptic class in four dimension. We call the final perturbations as Quantum perturbation analysis due to the fact that we are able to explore the entire range of linearized perturbation functions including from analysing just b'_1 equation or just linearized f''_1 equation or analysing both b'_1, f''_1 equations simultaneously.

This method can be worked out as an extensive method that holds for all dimensions and all matter content as well. Some of the steps are taken from [41] and [42] while making use of some algebraic computations we could remove $u(t, r)$ and its derivatives from all the equations ¹. One can perturb the exact solutions h_0 (where h denotes either b , or f) that are explored in Section 2 as follows

$$h(t, r) = h_0(z) + \varepsilon h_1(t, r) \quad (18)$$

where ε is a small number. By expanding equations in powers of ε , the zeroth order part results the background equations which has been studied in Section 2

¹Some similar perturbations of spherically symmetric solutions for Horava Gravity were carried out in [43].

and the linearized equations for the perturbations $h_1(t, r)$ are explored due to the linear terms in ε . One considers the perturbations of the form

$$h(z, t) = h_0(z) + \varepsilon(-t)^{-\kappa} h_1(z), \quad (19)$$

Since four dimensional axion-dilaton system was known to be stable, we assume the same holds for all other cases and take into account $\text{Re } \kappa > 0$. We are able to explore the spectrum of κ by solving the equations for $h_1(z)$. Indeed one can point out that the general solution to the first-order equations will be gained just with the linear combination of these modes. We would like to find out the mode κ^* with the biggest real part (by assuming a growing mode which would be $t \rightarrow 0$, i.e $\text{Re } \kappa > 0$) which will be related to critical Choptuik exponent as [5, 15, 17]

$$\gamma = \frac{1}{\text{Re } \kappa^*} \quad (20)$$

We consider only real modes κ^* where the values $\kappa = 0$ and $\kappa = 1$ are indeed gauge modes with respect to phase of f or $U(1)$ re-definitions of f and time translations as well [28] where these modes have been eliminated from the calculations.

3.1 Perturbation Equations in 4D For the Elliptic Class

The method for deriving the perturbations has been explained in [28], however since we want to analyse the Quantum perturbation analysis, exploring the entire range of perturbation functions including from just b'_1 just f''_1 as well as analysis of both b'_1, f''_1 simultaneously.

Indeed, here unlike the all literature we explore the whole (possible) range of possible values of critical exponents based on quantum perturbation theory. In fact we have analysed not only based on the perturbed DE variables $b_1(z)$, and the perturbed DE variables $f_{1m}(z) = g_m(z)$ but also on analysing DE variable of both $b_1(z), g_m(z)$ equations together as well to actually accept or reject the transitions under the Uniform prior distribution.

We therefore highlight briefly all perturbation equations as well. The perturbation ansatz (19), for b, τ functions are

$$b(t, r) = b_0(z) + \varepsilon(-t)^{-\kappa} b_1(z), \quad (21)$$

$$\tau(t, r) = i \frac{1 - (-t)^{i\omega} f(t, r)}{1 + (-t)^{i\omega} f(t, r)}, \quad (22)$$

$$f(t, r) \equiv f_0(z) + \varepsilon(-t)^{-\kappa} f_1(z). \quad (23)$$

Using the ansätze (21) for the metric functions, one does calculate the Ricci tensor for the metric as a function of ε . We are able to find the zeroth-order and first-order parts from the limiting behaviors as follows

$$R_{ab}^{(0)} = \lim_{\varepsilon \rightarrow 0} R_{ab}(\varepsilon) \quad R_{ab}^{(1)} = \lim_{\varepsilon \rightarrow 0} \frac{dR_{ab}(\varepsilon)}{d\varepsilon}. \quad (24)$$

The same method is carried out with the right-hand side \tilde{T}_{ab} of the field equations which means that

$$\tilde{T}_{ab}^{(0)} = \lim_{\varepsilon \rightarrow 0} \tilde{T}_{ab}(\varepsilon) \quad \tilde{T}_{ab}^{(1)} = \lim_{\varepsilon \rightarrow 0} \frac{d\tilde{T}_{ab}(\varepsilon)}{d\varepsilon}. \quad (25)$$

Indeed the Einstein Field Equations (EFEs) is held order by order so that

$$R_{ab}^{(0)} = \tilde{T}_{ab}^{(0)}, \quad R_{ab}^{(1)} = \tilde{T}_{ab}^{(1)}. \quad (26)$$

As explained, one can remove u and its first derivative in terms of b_0 , f and their first derivatives. We now combine the field equations so that we would be able to eliminate the second-derivative terms in $b(t, r)$. This procedure is known as Hamiltonian constraint, which can be shown by

$$C(\varepsilon) \equiv R_{tt} + b^2 R_{rr} - \tilde{T}_{tt} - b^2 \tilde{T}_{rr} = 0. \quad (27)$$

One finds the lowest-order contribution as a first-order equation relating b'_0 to b_0 , f_0 , f'_0 as follows

$$b'_0 = \frac{((z^2 - b_0^2)f'_0(z\bar{f}'_0 + i\omega\bar{f}_0) + \omega f_0(\omega z\bar{f}_0 - i(z^2 - b_0^2)\bar{f}'_0))}{b_0(1 - f_0\bar{f}_0)^2}. \quad (28)$$

In a similar method the first correction reads as

$$\left. \frac{dC(\varepsilon)}{d\varepsilon} \right|_{\varepsilon=0} = 0, \quad (29)$$

which is a first-order equation relating b'_1 to b_0 , b'_0 , f_0 , f'_0 , f''_0 , and the other perturbations b_1 , f_1 , f'_1 , which are indeed linear in all perturbations. For the

elliptic class in 4d one obtains the linearized equations for b'_1 as follows

$$\begin{aligned}
(L_1)b'_1 = & rt((t-2t)b_0 + rb'_0) \left(-\frac{2f'_1\bar{f}'_0r^2}{t^4s_0^2} - \frac{2b_1b'_0}{rt} + \frac{\kappa 2b_0b_1b'_0}{r((t-2t)b_0 + rb'_0)} \right. \\
& - \frac{4i\omega b_0b_1\bar{f}_0f'_0}{rts_0^2} + \frac{2i\omega b_0^2\bar{f}_1f'_0}{rts_0^3} + \frac{2\kappa\bar{f}_1f'_0r}{t^3s_0^2} + \frac{2i\omega\bar{f}_1f'_0r}{t^3s_0^2} \\
& - \frac{2\kappa b_0^2\bar{f}_1f'_0}{rts_0^2} + \frac{2i\omega\bar{f}_0f'_1r}{t^3s_0^2} - \frac{2i\omega b_0^2\bar{f}_0f'_1}{rts_0^2} + \frac{4b_0b_1f'_0\bar{f}'_0}{t^2s_0^2} \\
& + \frac{2b_0^2f'_1\bar{f}'_0}{t^2s_0^2} + \frac{1}{rt^4s_0^3} 2f_1 \left(t\omega\bar{f}_0^2(rt(-i\kappa + \omega)f_0 - 2i(r^2 - t^2b_0^2)f'_0) \right. \\
& + t(\kappa - i\omega)(-r^2 + t^2b_0^2)\bar{f}'_0 + \bar{f}_0(rt^2\omega(i\kappa + \omega) + t(\kappa + i\omega)) \\
& \times (r^2 - t^2b_0^2)f_0\bar{f}'_0 + 2r(r^2 - t^2b_0^2)f'_0\bar{f}'_0) \left. \right) - \frac{2f'_0\bar{f}'_1r^2}{t^4s_0^2} + \frac{2b_0^2f_0\bar{f}'_1}{t^2s_0^2} \\
& - \frac{2if_0(\bar{f}_1(r\omega t^2(\kappa + i\omega) + \omega t(2r^2 - t^2b_0^2)\bar{f}_0f'_0 + 2ir(r^2 - t^2b_0^2)f'_0\bar{f}'_0))}{rt^4s_0^3} \\
& - \frac{2if_0t\omega(-\bar{f}'_1r^2 + 2t^2b_0b_1\bar{f}'_0 + t^2b_0^2\bar{f}'_1)}{rt^4s_0^3} + \frac{4i\omega f_0^2(r^2 - t^2b_0^2)\bar{f}_1\bar{f}'_0}{rt^3s_0^3} \\
& \left. + \frac{2i\omega f_0^2(\bar{f}_0(-\bar{f}'_1r^2 + t(\kappa - i\omega)\bar{f}_1r + 2t^2b_0b_1\bar{f}'_0 + t^2b_0^2\bar{f}'_1))}{rt^3s_0^3} \right), \tag{30}
\end{aligned}$$

where

$$L_1 = 2b_0((\kappa - 1)tb_0 + rb'_0), \quad s_0 = (f_0\bar{f}_0 - 1). \tag{31}$$

Eq. (30) it is clearly invariant under dilations $(t, r) \rightarrow (e^\lambda r, e^\lambda t)$, so that, by changing coordinates to (t, z) , one finds that all the factors of t will cancel off and the final result just depends on z . Hence, we are left with just real and linear ordinary differential equation.

If we apply the perturbation ansätze in the τ equation of motion (7) and extract the zeroth and first-order parts and remove all u'_0, u_1, u'_1 , then the resulting zeroth-order part will be an equation including $b_0, b'_0, f_0, f'_0, f''_0$, while substituting b'_0 according to eq. (12) and solving for f''_0 , we obtain a second-order equation for f_0 , which is indeed the explicit form of eq. (13): Once more the first-order part includes $b_1, b'_1, f_1, f'_1, f''_1$ linearly, while the equations depend on the zeroth-order functions and their derivatives non-linearly as back ground

functions. Hence, we are left with the perturbations for f_1'' as follows

$$\begin{aligned}
(L_3)f_1'' = & r^2 \left(it\omega f_0^2 (\bar{f}_1 b_0' + \bar{f}_0 b_1') + f_1 b_0' (\kappa t - it\omega - t(\kappa - 2i\omega) f_0 \bar{f}_0 + r f_0' \bar{f}_0) \right. \\
& \left. - r(b_1' f_0' + b_0' f_1') + f_0 (b_1' (-it\omega + r \bar{f}_0 f_0') + r b_0' (\bar{f}_1 f_0' + \bar{f}_0 f_1')) \right) \\
& + r t^2 b_0^2 (f_1 \bar{f}_0 b_0' f_0' - b_1' f_0' - b_0' f_1' + f_0 (\bar{f}_1 b_0' f_0' + \bar{f}_0 (b_1' f_0' + b_0' f_1'))) \\
& - t^2 b_0^3 \left(2r \bar{f}_1 f_0'^2 - 2t f_1' + 4r \bar{f}_0 f_0' f_1' + f_1 \bar{f}_0 (2t f_0' - r f_0'') \right. \\
& \left. + f_0 (2t \bar{f}_0 f_1' + \bar{f}_1 (2t f_0' - r f_0'')) \right) \\
& - r b_0 \left(t^2 \omega (\omega - i) f_0^2 \bar{f}_1 + 2r (-r \bar{f}_1 f_0'^2 + (t(1 + \kappa - i\omega) - 2r \bar{f}_0 f_0') f_1') \right. \\
& \left. + f_1 \left(t^2 (-\kappa^2 + \kappa(-1 + 2i\omega) + \omega(i + \omega)) + t^2 (\kappa + \kappa^2 + 2i\kappa\omega) \right. \right. \\
& \left. \left. + 2\omega(-i + \omega) \right) \bar{f}_0 f_0 + r \bar{f}_0 (2t(-1 + 2\kappa - i\omega) f_0' + r f_0'') \right) \\
& \left. + r f_0 (-2t(1 + \kappa + i\omega) \bar{f}_0 f_1' + \bar{f}_1 (-2it(-i + \omega) f_0' + r f_0'')) \right) \\
& - b_1 \left(r t^2 \omega (-i + i\kappa + \omega) f_0^2 \bar{f}_0 - t(r^2(-2 + \kappa + 2i\omega) + 6t^2 b_0^2) \right. \\
& - 2r t b_0 b_0' f_0' - 2r(r^2 - 3t^2 b_0^2) \bar{f}_0 f_0'^2 - r(r^2 - 3t^2 b_0^2) f_0'' \\
& + f_0 \left(r t^2 \omega (i - i\kappa + \omega) + \bar{f}_0 (t(r^2(-2 + \kappa - 2i\omega) + 6t^2 b_0^2) \right. \\
& \left. \left. - 2r t b_0 b_0' f_0' + r(r^2 - 3t^2 b_0^2) f_0'') \right) \right), \tag{32}
\end{aligned}$$

where

$$L_3 = r b_0 (r^2 - t^2 b_0^2) s_0. \tag{33}$$

Above equations are scale-invariant, hence they turn to an ordinary differential equation after making use of a change of coordinates to (z, t) . Hence we are left with a system of ordinary linear differential equations as

$$b_1' = B_1(b_1, f_1, f_1'), \tag{34}$$

$$f_1'' = F_1(b_1, f_1, f_1'). \tag{35}$$

Notice that as a matter of fact B_1 and F_1 are indeed now linear functions that still depend non-linearly on the unperturbed solution. We also have a quadratic dependence on κ as well. Note that these equations also do include the same

singularities as appeared in the unperturbed system of equations which means that they are also singular for $z = 0$ and $b^2(z) = z^2$. The modes are now explored by finding the κ values that are related to smooth solutions of the perturbed equations (34), (35) where they need to satisfy the proper boundary conditions as follows.

4 Procedure For Perturbations

We now turn to boundary conditions needed to solve Eqs. (34), (35). First of all at $z = 0$ we re-scale the time coordinate, so that $b_1(0) = 0$, and also using the regularity condition for the axion-dilaton at $z = 0$ we find that $f_1'(0) = 0$ so that the freedom in f is reduced to $f_1(0)$ which is an unknown complex parameter. We also demand that at z_+ (we recall that z_+ is defined by the equation $b(z_+) = z_+$) all equations and perturbations be regular so that all the second derivatives $\partial_r^2 f(t, r)$, $\partial_r \partial_t f(t, r)$, $\partial_t^2 f(t, r)$ should be finite as $z \rightarrow z_+$. Hence, $f_0''(z)$ and $f_1''(z)$ are also finite as $z \rightarrow z_+$. We introduce $\beta = b_0(z) - z$ and then expand f_0'' , f_1'' near the singularity, as

$$f_0''(\beta) = \frac{1}{\beta} G(h_0) + \mathcal{O}(1), \quad (36)$$

$$f_1''(\beta) = \frac{1}{\beta^2} \bar{G}(h_0) + \frac{1}{\beta} H(h_0, h_1|\kappa) + \mathcal{O}(1), \quad (37)$$

where we have defined the following equations

$$h_0 = (b_0(z_+), f_0(z_+), f_0'(z_+)), \quad h_1 = (b_1(z_+), f_1(z_+), f_1'(z_+)) \quad (38)$$

The vanishing unperturbed complex constraint is given by $G(h_0) = 0$ at z_+ , and we checked that it implies $\bar{G}(h_0) = 0$ at z_+ as well, which means that

$$G(h_0) = 0 \Rightarrow \bar{G}(h_0) = 0, \quad (39)$$

Hence we are left just with the complex-valued constraint

$$H(h_0, h_1|\kappa) = 0, \quad (40)$$

that is linear in h_1 .

We now try to solve this constraint for $f_1'(z_+)$ in terms of $f_1(z_+)$, $b_1(z_+)$, κ and h_0 . Hence, this condition reduces the number of free parameters in the boundary conditions at z_+ to a real number $b_1(z_+)$ and a complex $f_1(z_+)$. In conclusion, we have six real unknowns, which are κ and the five-component vector as

$$X = (\text{Re } f_1(0), \text{Im } f_1(0), \text{Re } f_1(z_+), \text{Im } f_1(z_+), b_1(z_+)) \quad (41)$$

and the system of linear ODE's eqs. (34), (35) whose total real order is indeed five. Let us now briefly explain the numerical procedure that was used in [28]. Given a set of boundary conditions X , we integrate from $z = 0$ to an intermediate point z_{mid} and similarly we integrate backwards from z_+ to z_{mid} . Finally we collect the values of all functions ($b_1, \text{Re } f_1, \text{Im } f_1, \text{Re } f_1', \text{Im } f_1'$) at z_{mid} and encode the difference between the two integrations in a “difference function” $D(\kappa; X)$. By definition, $D(\kappa; X)$ is linear in X thus it has a representation as a matrix form

$$D(\kappa; X) = A(\kappa)X \quad (42)$$

where $A(\kappa)$ is a 5×5 real matrix depending on κ . So we need to just find the zeroes of $D(\kappa; X)$ and this can be achieved by evaluating $\det A(\kappa) = 0$. We carry out the root search for the determinant as a function of κ where the root with the biggest value will be related to the Choptuik exponent through eq. (20). It is worth highlighting one last point. The perturbed equations of motion are singular whenever the factor $(\kappa - 1 - z \frac{b_0'}{b_0})$ in the denominator vanishes, so that the numerical procedure fails at particular point. We can get an estimate for the values of κ giving rise to this singular behaviour and we can also find the entire region which leads to numerical failure. However, this apparent problem does not affect our evaluation of the critical exponent because in most cases the most relevant mode κ^* lies outside that particular failure region.

5 Statistical Methods

In this section, we propose various statistical methods to optimize the equations of motion, estimate the parameters of the differential equations, and use the Bayesian approach to find the posterior distributions of critical exponents in the equations of motion. We describe polynomial regression models in subsection 5.1, artificial neural networks in subsection 5.2 and the Markov Chain Monte

Carlo for Bayesian estimation in subsection 5.3.

5.1 Polynomial Regression Method

Polynomial regression models are established tools in data science to model multivariate data and find the relationship between variables. Let (\mathbf{x}, \mathbf{Z}) be the input multivariate data, where \mathbf{x} denotes the response vector of sample size n and \mathbf{Z} denotes the design matrix of size $(n \times p)$ with p independent variables $(\mathbf{z}_1, \dots, \mathbf{z}_p)^\top$. Given the training data of size n , the multivariate regression

$$x_i = \mathbf{z}_i^\top \beta + \epsilon_i, \quad (43)$$

where ϵ_i are independent and identically distributed (id) variables from the standard Gaussian distribution; that is, $N(0, 1)$.

The regression model (43) essentially converts predicting the response differential equation variable $x = g(\mathbf{z})$ into estimating the unknown coefficients of the model. The least squares (LS) method is a common approach to estimating the regression model coefficients (43) minimizing the l_2 norm between the predicted responses and observed responses as

$$\hat{\beta} = \arg \min_{\beta} \|\mathbf{x} - \mathbf{Z}\beta\|_2^2. \quad (44)$$

One can easily show that the LS estimate of unknown coefficients can be obtained by $\hat{\beta}_{LS} = (\mathbf{Z}^\top \mathbf{Z})^{-1} \mathbf{Z}^\top \mathbf{x}$ as the solution to (44). Hence, the differential equation response $x(z)$ at every space-time point z_{new} is predicted by $\hat{x}_{new} = \mathbf{z}_{new} \hat{\beta}_{LS}$ [44].

The polynomial regression model extends the properties of multivariate regression by employing the higher-order terms of the independent variables to better predict the nonlinear pattern of the response function $x = g(z)$. The polynomial regression of order J is given by

$$x_i = \sum_{j=1}^J z_i^j \beta_j + \epsilon_i, \quad (45)$$

where $\beta = (\beta_1, \dots, \beta_J)$ are the model coefficients that should be estimated. One can easily represent (45) in matrix form as (43) where the columns of the design matrix \mathbf{Z} induce the explanatory variable $z_i, i = 1, \dots, n$ raised to various polynomial powers $j = 1, \dots, J$. From the least squares method (44), one can

predict the non-linear responses of the differential equations at every point z_{new} in the domain of the equations of motion by $\hat{x}_{new} = \mathbf{z}_{new}\hat{\beta}_{LS}$.

5.2 Artificial Neural Networks

In this subsection, we follow the idea of artificial neural networks to numerically find the gravitational critical collapse functions from perturbed equations of motion.

The artificial neural networks encompass multi-layer perceptrons, transferring data between the layers through linear and non-linear functions. Various neural networks have been developed in the literature, including, for instance, convolutional neural networks and recursive neural networks, where each is suited to different applications across numerous scientific areas. In this research, we focus on fully connected neural networks to deal with the non-linearity of the elliptic perturbed equations of motion in the Einestain-axion-delation system in 4D.

Let $\mathcal{N}^L(\mathbf{x}, t, \psi)$ denote a neural networks with L layers which map the input dimensions R^{in} to R^{out} . Let \mathbf{W}^l and \mathbf{b}^l denote the weight matrix and bias vector, which regress the neurons in layer l on $l - 1$, respectively. Accordingly, the response vector before activation in layer l is given by

$$y^l = \mathbf{W}^l N^{l-1}(\mathbf{x}, t, \psi) + \mathbf{b}^l, \quad (46)$$

where the output of layer l is obtained after applying the activation function, that is $N^l(\mathbf{x}, t, \psi) = \eta(y^l)$, $l = 1, \dots, L - 1$.

The universal approximation theorem guarantees that the neural networks can approximate any function, making the neural networks a state-of-the-art method for solving nonlinear equations [45]. One must define a loss function \mathcal{L} to assess the performance of the ANNs and a back-propagation algorithm to adjust the weight matrices and bias parameters of the ANN based on the gradient of the loss functions. The back-propagation algorithm calculates the gradients of the ANNs with respect to the response variable to ensure that the estimates of the ANN's coefficients meet the requirements of the loss function. This process translates solving the differential equations of motion into an optimization problem, estimating the differential variables based on minimizing the squared residues of the ANNs. Accordingly, for this purpose, we introduce the l_2 loss function as

$$\mathcal{L}(\mathcal{N}^L(\mathbf{x}, t, \psi)) = (\mathcal{N}^L(\mathbf{x}, t, \psi) - g)^2,$$

where $\mathcal{N}^L(\mathbf{x}, t, \psi)$ represents the trained neural networks approximating the underlying function. In this manuscript, we use the fully connected ANNs to solve the system of ordinary equations pertinent to the perturbed elliptic class of black hole equations of motion as an alternative method to general relativity-based methods.

5.3 Markov Chain Monte Carlo

Consider a system of H differential equations where $\mathbf{x}(t) = (x_1(t), \dots, x_H(t))$ represents the multivariate solutions evaluated at space-time t to the system of differential equations (DEs)

$$\frac{d}{dt}x_h(t) = g_h(\mathbf{x}(t)|\theta), \quad (47)$$

where the DE variable $x_h(t)$ corresponds to h DE and θ denotes the collection of the unknown parameters of the DE. Due to the high non-linearity of the black hole equations of motion, the exact solution to the DE equations can be observed. Rather than the exact DE solution, one may observe a perturbed version of the DE variable with numerical measurement errors through numerical experiments. To take this uncertainty into statistical methods, let $\mathbf{y}_h = (y_{h1}, \dots, y_{hn})$ denote the observed version of the DE variable $x_h(t)$ at n space-time points. Hence, let $y_{h,i}$ follow a Gaussian distribution with mean $x_h(t_i|\theta)$ and variance σ_h^2 . Given the Gaussian distribution of the observed data, the uncertainty in the DE data can be modelled by the likelihood function of y_i as

$$L(\theta|\mathbf{y}) = \prod_{h=1}^H \prod_{i=1}^n (1/\sigma_h^2) \exp\{- (y_{hi} - x_h(t_i|\theta))/2\sigma_h^2\}, \quad (48)$$

The likelihood function translates the problem of finding the solution to a system of DEs into a Gaussian process with unknown parameters. One can estimate the unknown parameters of the DE system given the observed DE variables by maximizing the likelihood function.

According to the non-linear nature of the DE variables, the likelihood function (48) appears nonlinear with multiple optimums, indicating the sensitivity of the maximum likelihood estimate of the DE variables.

Here, we propose a Bayesian approach incorporating the numerical measurement errors in estimating the critical exponent parameter in the DE equation

of motion (34),(35). This framework requires prior knowledge of model parameters. This prior knowledge is incorporated into equations through a prior probability density function. Let $\pi(\theta; \alpha)$ denote this prior distribution, with α representing the vector of hyper-parameters.

Using information contained in the likelihood function (48) and the prior distribution, one can find the posterior distribution of the unknown parameters $\pi(\theta|\mathbf{y})$. The posterior distribution enables u to capture the pattern of the parameters of the DE system using all the uncertainty involved in calculating the DE variables. The posterior distribution of θ is calculated by

$$\pi(\theta|\mathbf{y}) = \frac{L(\theta|\mathbf{y})\pi(\theta; \alpha)}{\int_{\theta} L(\theta|\mathbf{y})\pi(\theta; \alpha)}. \quad (49)$$

Nevertheless, the posterior distribution (49) lacks a closed-form solution because of the high non-linearity of the DE variables and the complex marginal distributions of the DE variables. For this reason, one has to use iterative methods such as Markov Chain Monte Carlo to find numerically the posterior distribution of the parameters of the DE system [46].

Markov Chain Monte Carlo (MCMC) is a widely acceptable numerical technique within the Bayesian framework to estimate the posterior distribution of the DE system. The power of the MCMC approach relies on the fact that it transfers the estimation task into the sampling process from the posterior distribution of the interest [47]. Extensive research has been conducted in the literature about the properties of the MCMC approach, including Metropolis-Hastings, Gibbs sampling, and Sequential Monte Carlo. In its nutshell, MCMC employs various probabilistic techniques to generate a march chain of samples approximating the target posterior distribution. When the chain is selected long enough, the Markov chain will eventually reach a stationary state that accurately fluctuates around the true form of the posterior distribution.

Metropolis-Hastings (MH) is an established MCMC approach. The MH method calculates the probability of the transition between the current state of the chain $\theta^{(t)}$ and a candidate state θ^* simulated stochastically from an independent proposal distribution $q(\theta)$. The MH method applies a probabilistic step to accept or reject the proposed candidate.

let $\theta^{(t)}$ represent the t -th state of the MCMC chain. Then we accept the

proposed state θ^* as the next state of the chain with probability

$$\min \left\{ 1, \frac{\pi(\theta^*|\mathbf{y})q(\theta^{(t)})}{\pi(\theta^{(t)}|\mathbf{y})q(\theta^*)} \right\}. \quad (50)$$

If the candidate θ^* is accepted, then $\theta^{(t+1)} = \theta^*$; otherwise, $\theta^{(t+1)} = \theta^{(t)}$. The entire MCMC method is replicated N times to generate a sequence of $\{\theta^{(t)}; t = 1, \dots, N\}$ samples from the target posterior distribution $\pi(\theta|\mathbf{y})$.

6 Numerical Studies

In this section, we plan to find the distribution of the critical exponent κ in the elliptic 4D equations of motion in the Bayesian framework. To do so, the critical exponent is treated as a random variable, so we use the Bayesian strategy to find the posterior distribution of κ based on the perturbed DE system. In this numerical study, we investigate the equations of motion as the input DE system. Hatefi et al. (2023) in [32] proposed ANNs to solve the unperturbed DE variable. We applied the properties of polynomial regression and found the closed-form polynomial regression estimates for the unperturbed critical collapse functions. According to the fact that the goal of this research is to estimate the critical exponent and that the critical exponent is only observed in perturbed DE variables, we first followed [32] and used the ANNs based on $\omega = 1.176$ to numerically find the unperturbed critical collapse functions in the entire domain of the DE system. To find the regression estimate of the unperturbed critical collapse functions, we generated equally spaced points z_1, \dots, z_n of size $n = 1000$ from the domain of the DE system. We then obtained the ANN estimates of the unperturbed critical collapse functions evaluated at each of the 1000 points. Once we obtained the ANN estimates, we used 750 observations as training and 250 as testing data to estimate the closed-form polynomial regression of the unperturbed critical collapse functions. Hence, the closed-form polynomial estimates of the unperturbed critical collapse functions are derived by

$$\begin{aligned} \widehat{b_0(z)} &= 1.005 - 0.187z + 0.480z^2 - 0.004z^3, \\ |\widehat{f_0(z)}| &= 0.919 - 0.122z - 0.028z^2 - 0.002z^3, \\ \arg(\widehat{f_0(z)}) &= -0.011 + 0.041z + 0.047z^2 - 0.012z^3, \end{aligned}$$

Figure 1 shows the training and test performance of the polynomial estimates

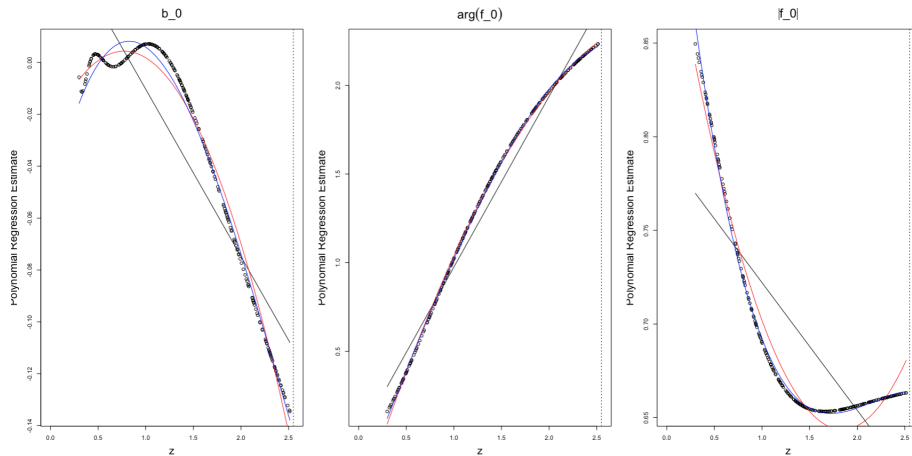


Figure 1: The polynomial estimates of the unperturbed critical collapse functions $b_0(z)$, $\arg(f_0(z))$ and $|f_0(z)|$ of the equations of motion based on polynomial orders of $l = 1$ (black), $l = 2$ (red) and $l = 3$ (blue). The dots show the functions evaluated at the validation points.

for the critical collapse functions for polynomial orders $l = 1, 2, 3$. One can easily see that the polynomial of order $l = 3$ can capture very well the nonlinearity of the unperturbed critical collapse functions. Once we found the unperturbed DE variables $b_0(z)$, $|f_0(z)|$ and $\arg(f_0(z))$, we incorporated these estimates and updated the perturbed equations of motion. In the next step, we consider this perturbed equations of motion, as our underlying DE system to estimate the critical exponent.

We proposed an artificial neural network-assisted Metropolis-Hastings to obtain the posterior distribution of κ . To do so, we first generated κ candidates from a proposal distribution. Here, we considered two proposal distributions, including the Uniform distribution between (3,4) and the Gaussian distribution with a mean of 3.5 and variance of 1. In the next step, we apply fully connected neural networks using the κ candidate and find the solution to the perturbed equations of motion corresponding to the κ candidate. Here, we applied a fully connected neural network with 4 hidden layers, each layer with 16 neurons and 50 epochs. We then computed the likelihood function (48) and found the acceptance probability of the Metropolis-Hasting algorithm. Due to the fact that the range of DE variables is dramatically different, we assign $\sigma_{b_1} = 7$ and $\sigma_g = 2$ in the likelihood function of κ given the perturbed DE variables.

It is shown in the literature that the perturbed $b_1(z)$ DE variable is linear

with respect to κ ; however, the perturbed $g_m(z)$ contains the higher orders of κ [28]. To investigate the effects of the different DE variables on the MCMC chains and the Bayesian distribution of the κ , we evaluated the performance of the stochastic accept-reject method based on three scenarios. These scenarios include the accept-reject step based on only the observed perturbed DE variable of $b_1(z)$, accept-reject based on only the observed perturbed DE variable $g_m(z)$ and accept-reject based on both observed perturbed DE variables $g_m(z)$ and $b_1(z)$. Finally, the entire neural network-assisted Metropolis-Hasting approach was carried out for 2000 chains, where in each iteration, the perturbed equations of motion were computed using artificial neural networks. We discard the first 10% of the history of the MCMC chain to wash out the effect of the initialization step on the performance of the MCMC chain.

Figures 2-7 show the posterior distributions and trace plots of the κ parameter based on 1800 MCMC chains (after discarding the burn-in period) using the artificial neural networks-assisted Metropolis-Hastings. The results are based on three accept-reject approaches and two proposal distributions, including uniform and Gaussian distributions. From Figures 2-7, we observe that the posterior distributions appear almost bimodal, which is consistent with the finding in the literature that the equations of motion consist of the κ and κ^2 parameters. We also observe that the distribution's posterior mean and posterior mode, as two Bayesian estimates of the κ range between 3.2 and 3.8 which verifies the findings in the literature that $\kappa^* \approx 3.7858$ for the equations of motion in 4D elliptic class. From the trace plot, we easily observed that the MCMC chain easily searches the domain of the parameter of interest and supports the solution between 3.2 and 3.8.

As one needs the ANNs in each iteration of the MCMC chain to evaluate the accept-reject steps, we show the results of the loss function of ANNs in Figures 8-10. Due to the similarity between the results, we only showed the performance of the loss function under uniform proposal distribution in the appendix. To show the convergence of the ANNs, we computed the difference between training and validation loss functions in the last epoch of the ANNs over 1800 MCMC samples. In each figure, we also show the entire trajectory of the training and validation loss functions over all the epochs for a randomly selected MCMC sample. From Figures 8-10, we clearly observe the loss differences are almost very small of magnitude 10^{-6} fluctuating around zero. This highlights the convergence of the ANNs in estimating the critical exponent in a Bayesian framework.

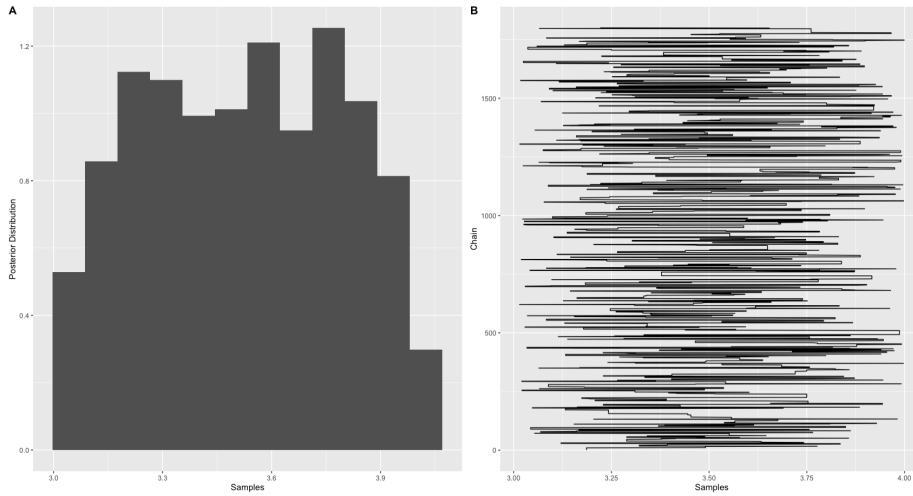


Figure 2: The posterior distribution and trace plot of the κ based on 1800 MCMC samples from the Metropolis-Hastings using only the perturbed DE variable $b_1(z)$ to accept or reject the transitions under the Uniform prior distribution.

The unique solution for the elliptic case in four dimensions was achieved in [28]. Indeed, the behaviour of $\det A(k)$ near the last crossing of the horizontal axis was estimated to be

$$\kappa_{4E}^* \approx 3.7858, \quad (51)$$

which gives rise to a Choptuik exponent as $\gamma_{4E} \approx 0.2641$. In this paper, we have used various statistical methods to actually explore the entire range of the critical exponent rather than exploring the last crossing. Surprisingly, our results

$$3.2 < \kappa_{4E}^* < 3.8 \quad (52)$$

is in perfect agreement with the literature, see [39]. Hence, we can actually take this very non-trivial match as evidence that shows all our numerical sets up are reliable methods that can be extended to any dimension and any matter content.

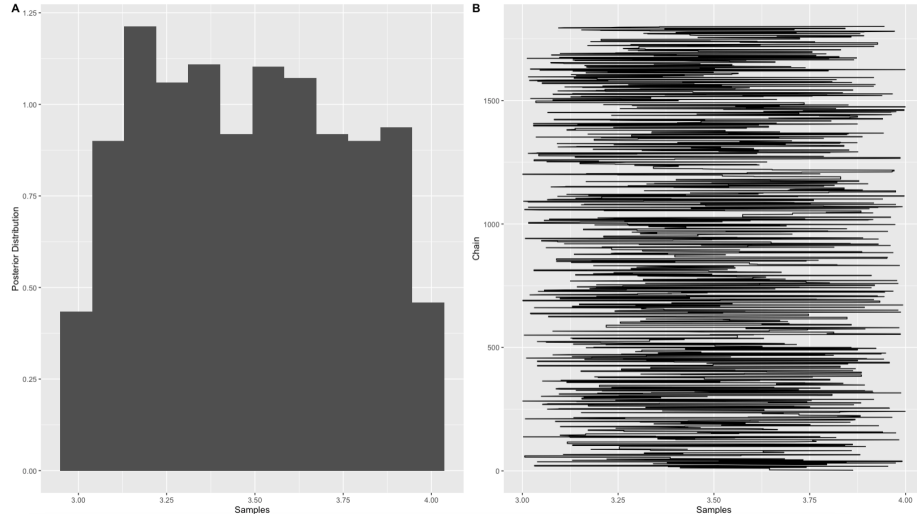


Figure 3: The posterior distribution and trace plot of the κ based on 1800 MCMC samples from the Metropolis-Hastings using only the perturbed DE variable $f_{1m}(z) = g_m(z)$ to accept or reject the transitions under the Uniform prior distribution.

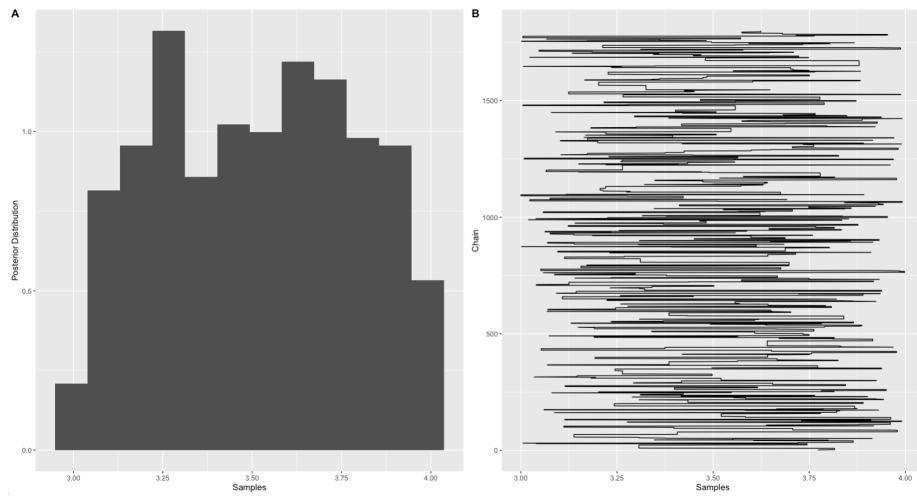


Figure 4: The posterior distribution and trace plot of the κ based on 1800 MCMC samples from the Metropolis-Hastings using both the perturbed DE variables $b_1(z)$ and $g_m(z)$ to accept or reject the transitions under the Uniform prior distribution.

7 Conclusion

In this paper, we enhanced the current literature on critical exponents for black hole solutions by exploring all the solutions in the entire domains of the linear perturbation equations. We explore the Quantum perturbation theory for four dimensional Einstein-axion-dilaton system of elliptic class of $SL(2, \mathbb{R})$ transformation. We have investigated neural networks assisted Metropolis-Hastings for Bayesian estimation of Critical exponent on elliptic Black Hole Solution in 4D Using Quantum Perturbation Theory. Indeed, unlike all literature we explored the whole (possible) range of possible values of critical exponents based on quantum perturbation theory. In fact we have analysed not only based on the perturbed DE variables $b_1(z)$, and the perturbed DE variables $f_{1m}(z) = g_m(z)$ but also on analysing DE variable of both $b_1(z), g_m(z)$ equations simultaneously to accept or reject the transitions under the Uniform prior distribution. Unlike methods in the literature, not only this new probabilistic approach provides us the available deterministic solution but also explore the entire range of physically distinguishable critical exponents that might occur due to numerical measurement errors.

These new methods open up new approaches towards exploring the possible range of the allowed values for critical exponent and it applied to all different conjugacy classes of the $SL(2, \mathbb{R})$ transformation. It is also important to highlight that these methods can be applied to some other matter content. This is a path that we would like to follow in the future.

In terms of results, what is interesting is that apart from the fact that the critical exponents depend on the matter content, dimension, and various solutions of self-critical collapse [25], they can also get the entire range of possibilities rather than having just an exact localised value. Hence, we conclude that the conjecture about the universality of Choptuik exponent is not satisfied. However, there might be some universal behaviours hidden in combinations of critical exponents and other parameters of the given theory that have not been taken into considerations by our current attempts. Based on our new analysis, we also provide clear evidence that transferring standard expectations of Statistical Mechanics from the critical gravitational collapse is not fulfilled.

8 Acknowledgments

E. Hatefi would like to thank Pablo Diaz, E. Hirschmann, Philip Siegmann, L. Alvarez-Gaume, and A. Sagnotti for useful discussions and supports. E. Hatefi is supported by the María Zambrano Grant of the Ministry of Universities of Spain. Armin Hatefi acknowledges the support from the Natural Sciences and Engineering Research Council of Canada (NSERC).

References

- [1] M.W. Choptuik, “Universality and Scaling in Gravitational Collapse of a Massless Scalar Field,” *Phys. Rev. Lett.* **70**, 9 (1993).
- [2] D. Christodoulou, “The Problem of a Self-gravitating Scalar Field,” *Commun. Math. Phys.* **105** (1986) 337; “Global Existence of Generalized Solutions of the Spherically Symmetric Einstein Scalar Equations in the Large,” *Commun. Math. Phys.* **106** (1986) 587; “The Structure and Uniqueness of Generalized Solutions of the Spherically Symmetric Einstein Scalar Equations,” *Commun. Math. Phys.* **109** (1987) 591.
- [3] R. S. Hamade and J. M. Stewart, “The Spherically symmetric collapse of a massless scalar field,” *Class. Quant. Grav.* **13** (1996) 497 [arXiv:gr-qc/9506044].
- [4] C. Gundlach, “Critical phenomena in gravitational collapse,” *Phys. Rept.* **376** (2003) 339 [gr-qc/0210101].
- [5] T. Koike, T. Hara, and S. Adachi, “Critical Behavior in Gravitational Collapse of Radiation Fluid: A Renormalization Group (Linear Perturbation) Analysis,” *Phys. Rev. Lett.* **74** (1995) 5170 [gr-qc/9503007].
- [6] L. Alvarez-Gaume, C. Gomez and M. A. Vazquez-Mozo, “Scaling Phenomena in Gravity from QCD,” *Phys. Lett. B* **649** (2007) 478 [hep-th/0611312].
- [7] M. Birukou, V. Husain, G. Kunstatter, E. Vaz and M. Olivier, “Scalar field collapse in any dimension,” *Phys. Rev. D* **65** (2002) 104036 [gr-qc/0201026].

- [8] V. Husain, G. Kunstatter, B. Preston and M. Birukou, “Anti-de Sitter gravitational collapse,” *Class. Quant. Grav.* **20** (2003) L23 [gr-qc/0210011].
- [9] E. Sorkin and Y. Oren, “On Choptuik’s scaling in higher dimensions,” *Phys. Rev. D* **71**, 124005 (2005) [arXiv:hep-th/0502034].
- [10] J. Bland, B. Preston, M. Becker, G. Kunstatter and V. Husain, “Dimension-dependence of the critical exponent in spherically symmetric gravitational collapse,” *Class. Quant. Grav.* **22** (2005) 5355 [gr-qc/0507088].
- [11] E. W. Hirschmann and D. M. Eardley, “Universal scaling and echoing in gravitational collapse of a complex scalar field,” *Phys. Rev. D* **51** (1995) 4198 [gr-qc/9412066].
- [12] J. V. Rocha and M. Tomašević, “Self-similarity in Einstein-Maxwell-dilaton theories and critical collapse,” *Phys. Rev. D* **98** (2018) no.10, 104063 [arXiv:1810.04907 [gr-qc]].
- [13] L. Alvarez-Gaume, C. Gomez, A. Sabio Vera, A. Tavanfar and M. A. Vazquez-Mozo, “Critical gravitational collapse: towards a holographic understanding of the Regge region,” *Nucl. Phys. B* **806** (2009) 327 [arXiv:0804.1464 [hep-th]].
- [14] C. R. Evans and J. S. Coleman, “Observation of critical phenomena and selfsimilarity in the gravitational collapse of radiation fluid,” *Phys. Rev. Lett.* **72** (1994) 1782 [gr-qc/9402041].
- [15] D. Maison, “Non-Universality of Critical Behaviour in Spherically Symmetric Gravitational Collapse,” *Phys. Lett. B* **366** (1996) 82 [gr-qc/9504008].
- [16] A. Strominger and L. Thorlacius, “Universality and scaling at the onset of quantum black hole formation,” *Phys. Rev. Lett.* **72** (1994) 1584 [hep-th/9312017].
- [17] E. W. Hirschmann and D. M. Eardley, “Critical exponents and stability at the black hole threshold for a complex scalar field,” *Phys. Rev. D* **52** (1995) 5850 [gr-qc/9506078].

- [18] A. M. Abrahams and C. R. Evans, “Critical behavior and scaling in vacuum axisymmetric gravitational collapse,” *Phys. Rev. Lett.* **70** (1993) 2980.
- [19] L. Alvarez-Gaume, C. Gomez, A. Sabio Vera, A. Tavanfar and M. A. Vazquez-Mozo, “Critical formation of trapped surfaces in the collision of gravitational shock waves,” *JHEP* **0902**, 009 (2009) [arXiv:0811.3969 [hep-th]].
- [20] E. W. Hirschmann and D. M. Eardley, “Criticality and bifurcation in the gravitational collapse of a selfcoupled scalar field,” *Phys. Rev. D* **56** (1997) 4696 [gr-qc/9511052].
- [21] J. M. Maldacena, “The Large N limit of superconformal field theories and supergravity,” *Int. J. Theor. Phys.* **38** (1999), 1113-1133, *Adv. Theor. Math. Phys.* **2**, arXiv:hep-th/9711200, E. Witten, “Anti-de Sitter space and holography,” *Adv. Theor. Math. Phys.* **2** (1998), 253-291, hep-th/9802150, S. Gubser, I. R. Klebanov and A. M. Polyakov, “Gauge theory correlators from noncritical string theory,” *Phys. Lett. B* **428** (1998), 105-114, hep-th/9802109.
- [22] D. Birmingham, “Choptuik scaling and quasinormal modes in the AdS / CFT correspondence,” *Phys. Rev. D* **64** (2001), 064024 [arXiv:hep-th/0101194 [hep-th]].
- [23] E. Hatefi, A. Nurmagambetov and I. Park, “ADM reduction of IIB on $\mathcal{H}^{p,q}$ to dS braneworld,” *JHEP* **04** (2013), 170, arXiv:1210.3825, “ N^3 entropy of $M5$ branes from dielectric effect,” *NPB* **866** (2013), 58-71, arXiv:1204.2711, S. de Alwis, R. Gupta, E. Hatefi and F. Quevedo, “Stability, Tunneling and Flux Changing de Sitter Transitions in the Large Volume String Scenario,” *JHEP* **11** (2013), 179, arXiv:1308.1222; E. Hatefi and I. Y. Park, *Phys. Rev. D* **85** (2012), 125039 [arXiv:1203.5553 [hep-th]]; E. Hatefi, *JHEP* **05** (2010), 080, [arXiv:1003.0314 [hep-th]].
- [24] E. Hatefi, *Phys. Rev. D* **86** (2012), 046003, [arXiv:1203.1329 [hep-th]]; E. Hatefi and I. Y. Park, *Nucl. Phys. B* **864** (2012), 640-663 [arXiv:1205.5079 [hep-th]]; E. Hatefi, *JCAP* **09** (2013), 011, [arXiv:1211.5538 [hep-th]]; E. Hatefi, *JHEP* **07** (2013), 002, [arXiv:1304.3711 [hep-th]]; E. Hatefi, *JHEP* **04** (2013), 070,

- [arXiv:1211.2413 [hep-th]]; E. Hatefi, *JHEP* **11** (2013), 204, [arXiv:1307.3520 [hep-th]].
- [25] R. Antonelli and E. Hatefi, “On self-similar axion-dilaton configurations,” , *JHEP* **03** (2020), 074 [arXiv:1912.00078 [hep-th]].
- [26] L. Álvarez-Gaumé and E. Hatefi, “Critical Collapse in the Axion-Dilaton System in Diverse Dimensions,” *Class. Quant. Grav.* **29** (2012) 025006 [arXiv:1108.0078 [gr-qc]].
- [27] L. Álvarez-Gaumé and E. Hatefi, “More On Critical Collapse of Axion-Dilaton System in Dimension Four,” *JCAP* **1310** (2013) 037 [arXiv:1307.1378 [gr-qc]].
- [28] R. Antonelli and E. Hatefi, “On Critical Exponents for Self-Similar Collapse,” *JHEP* **03** (2020), 180 [arXiv:1912.06103 [hep-th]].
- [29] E. Hatefi and A. Hatefi, “Estimation of Critical Collapse Solutions to Black Holes with Nonlinear Statistical Models,” *Mathematics* **10** (2022) no.23, 4537 [arXiv:2110.07153 [gr-qc]].
- [30] E. Hatefi and A. Hatefi, “Nonlinear statistical spline smoothers for critical spherical black hole solutions in 4-dimension,” *Annals Phys.* **446** (2022), 169112 [arXiv:2201.00949 [gr-qc]].
- [31] E. Hatefi, A. Hatefi and R. J. López-Sastre, “Analysis of black hole solutions in parabolic class using neural networks,” *Eur. Phys. J. C* **83** (2023) no.07, 623 [arXiv:2302.04619 [gr-qc]].
- [32] A. Hatefi, E. Hatefi and R. J. López-Sastre, “Modeling the complexity of elliptic black hole solution in 4D using Hamiltonian Monte Carlo with stacked neural networks,” *JHEP* **10** (2023), 034 [arXiv:2307.14515 [gr-qc]].
- [33] A. Hatefi and E. Hatefi, “Sequential Monte Carlo with cross-validated neural networks for complexity of hyperbolic black hole solutions in 4D,” *Eur. Phys. J. C* **83** (2023) no.11, 1083 [arXiv:2308.07907 [hep-th]].
- [34] A. Sen, “Strong - weak coupling duality in four-dimensional string theory,” *Int. J. Mod. Phys. A* **9** (1994) 3707 [hep-th/9402002].
- [35] J. H. Schwarz, “Evidence for nonperturbative string symmetries,” *Lett. Math. Phys.* **34** (1995) 309 [hep-th/9411178].

- [36] M.B. Green, J.H. Schwarz and E. Witten, 1987 Superstring Theory Vols I,II, Cambridge University Press,
- [37] J. Polchinski, 1998 String Theory, Vols I,II, Cambridge University Press
- [38] A. Font, L. E. Ibanez, D. Lust and F. Quevedo, “Strong - weak coupling duality and nonperturbative effects in string theory,” *Phys. Lett. B* **249** (1990) 35.
- [39] D. M. Eardley, E. W. Hirschmann and J. H. Horne, “S duality at the black hole threshold in gravitational collapse,” *Phys. Rev. D* **52** (1995) 5397 [arXiv:gr-qc/9505041].
- [40] E. Hatefi and E. Vanzan, “On Higher Dimensional Self-Similar Axion-Dilaton Solutions,” *Eur. Phys. J. C* **80** (2020), 10 [arXiv:2005.11646 [hep-th]].
- [41] R. S. Hamade, J. H. Horne and J. M. Stewart, “Continuous Self-Similarity and S -Duality,” *Class. Quant. Grav.* **13** (1996) 2241 [arXiv:gr-qc/9511024].
- [42] E. Hatefi and A. Kuntz, “On perturbation theory and critical exponents for self-similar systems,” *Eur. Phys. J. C* **81** (2021) no.15 [arXiv:2010.11603 [hep-th]].
- [43] A. Ghodsi and E. Hatefi, “Extremal rotating solutions in Horava Gravity,” *Phys. Rev. D* **81** (2010) 044016 [arXiv:0906.1237 [hep-th]].
- [44] F. Harrell Jr, “Regression modeling strategies: with applications to linear models, logistic and ordinal regression, and survival analysis,” Springer (2015).
- [45] Goodfellow, I., Bengio, Y., & Courville, A. “Deep learning”, MIT press. (2016)
- [46] Girolami, M. (2008). Bayesian inference for differential equations. *Theoretical Computer Science*, 408(1), 4-16.
- [47] Robert, C. P., Casella, G. (1999). Monte Carlo statistical methods (Vol. 2). New York: Springer.

Appendix

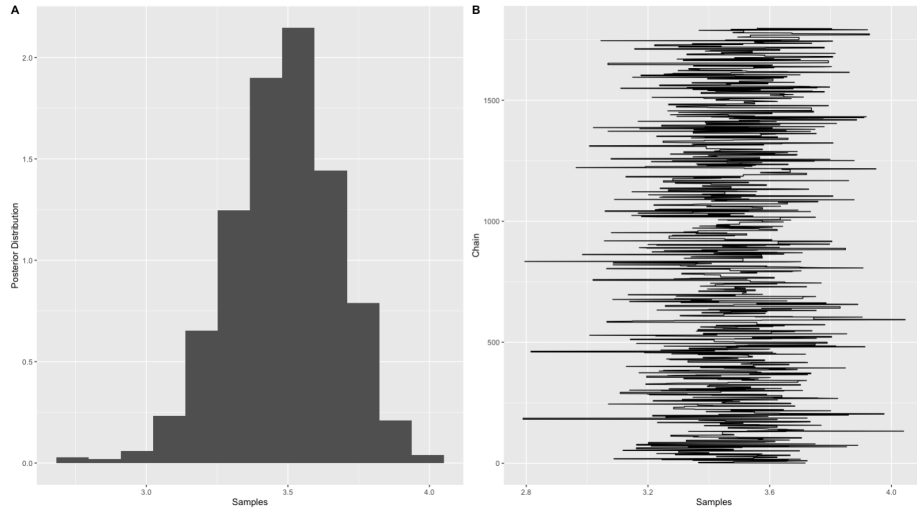


Figure 5: The posterior distribution and trace plot of the κ based on 1800 MCMC samples from the Metropolis-Hastings using only the perturbed DE variable $b_1(z)$ to accept or reject the transitions under the Gaussian prior distribution.

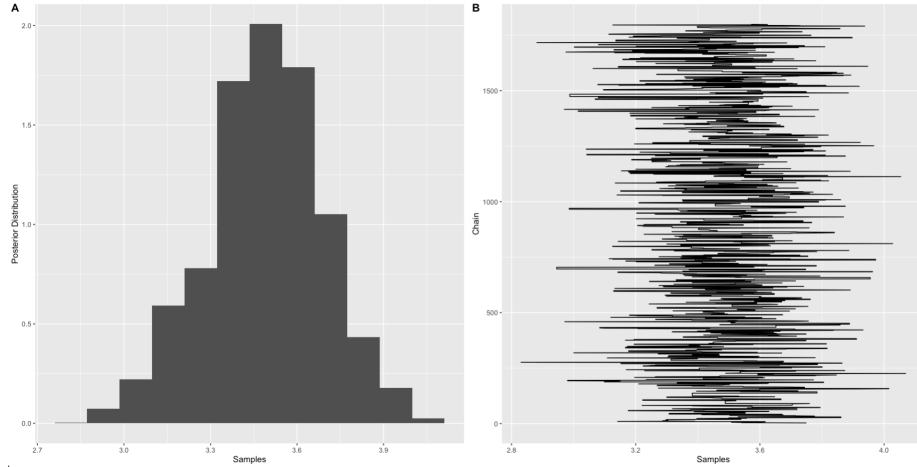


Figure 6: The posterior distribution and trace plot of the κ based on 1800 MCMC samples from the Metropolis-Hastings using only the perturbed DE variable $f_{1m}(z) = g_m(z)$ to accept or reject the transitions under the Gaussian prior distribution.

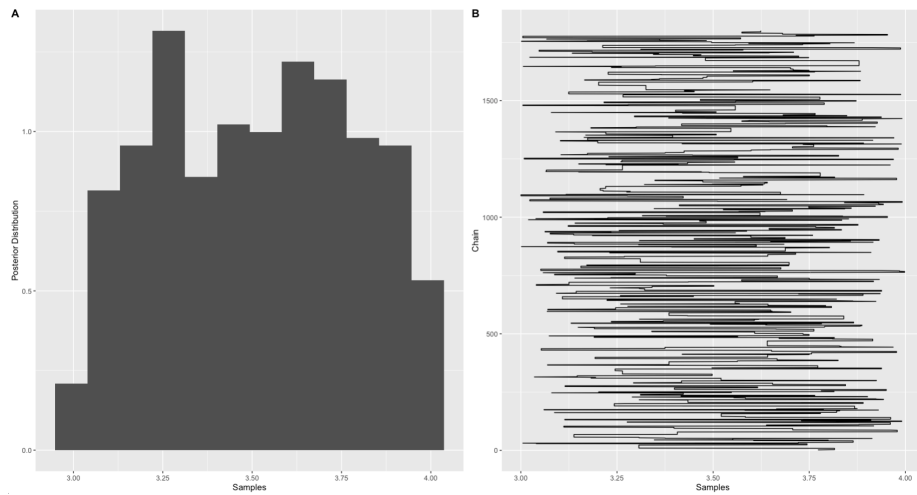


Figure 7: The posterior distribution and trace plot of the κ based on 1800 MCMC samples from the Metropolis-Hastings using both the perturbed DE variables $b_1(z)$ and $g_m(z)$ to accept or reject the transitions under the Gaussian prior distribution.

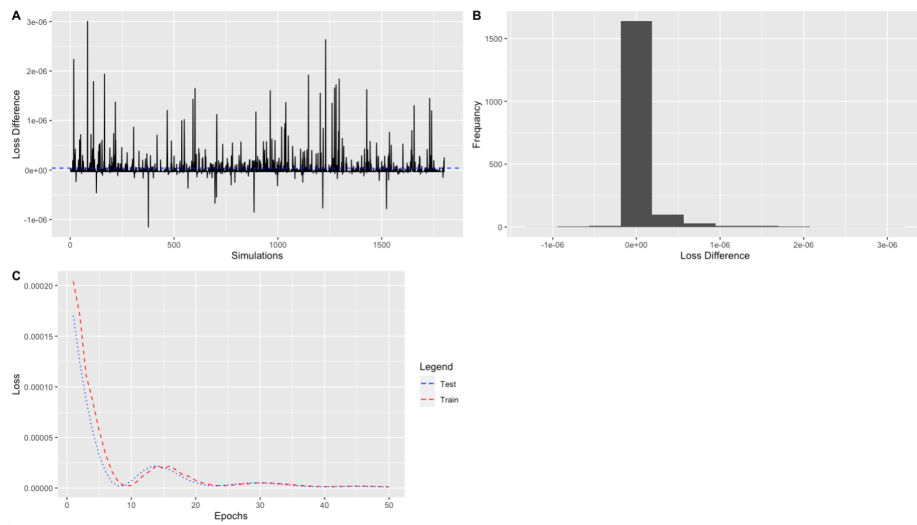


Figure 8: The difference between the train and validation losses in the last epochs over 1800 MCMC samples (A) and the histogram of the loss differences (B). The train and validation losses for one random MCMC sampling (C). The MCMC samples are from the Metropolis-Hastings using only the perturbed DE variable $b_1(z)$ to accept or reject the transitions under the Uniform prior distribution.

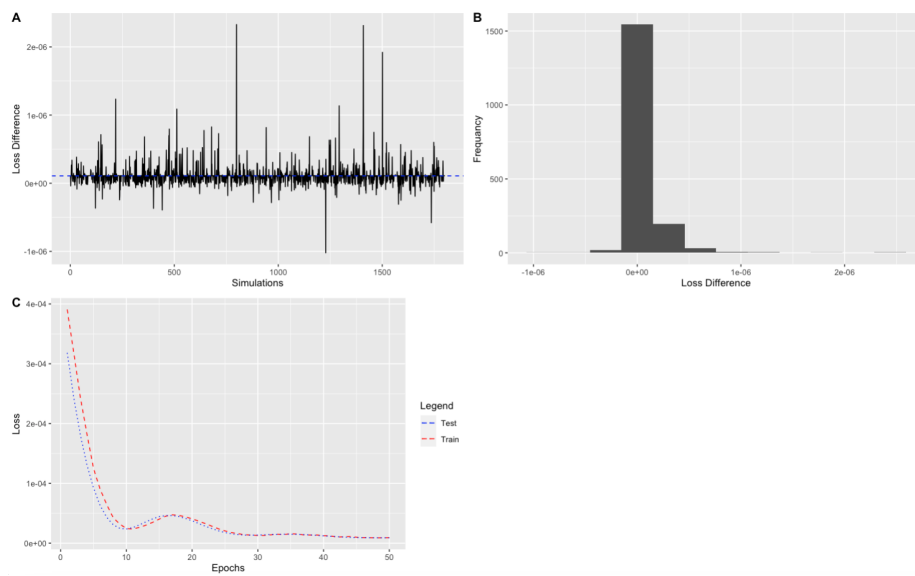


Figure 9: The difference between the train and validation losses in the last epochs over 1800 MCMC samples (A) and the histogram of the loss differences (B). The train and validation losses for one random MCMC sampling (C). The MCMC samples are from the Metropolis-Hastings using only the perturbed DE variable $g_m(z)$ to accept or reject the transitions under the Uniform prior distribution.

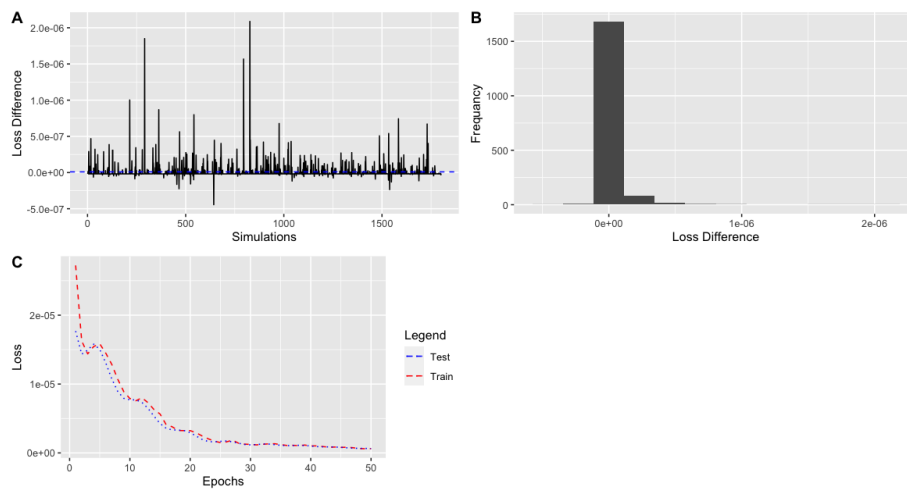


Figure 10: The difference between the train and validation losses in the last epochs over 1800 MCMC samples (A) and the histogram of the loss differences (B). The train and validation losses for one random MCMC sampling (C). The MCMC samples are from the Metropolis-Hastings using both perturbed DE variables $b_1(z)$ and $g_m(z)$ to accept or reject the transitions under the Uniform prior distribution.